Nucleic Acids Research, 2020 **1**
doi: 10.1093/nar/gkaa322

GSK-3 is an RNA polymerase II phospho-CTD kinase

Nicolás Nieto Moreno[1], Florencia Villafañez[2], Luciana E. Giono[1], Carmen Cuenca[1], Gastón Soria[2], Manuel J. Muñoz[1,3,4] and Alberto R. Kornblihtt[1,*]

[1]Departamento de Fisiología, Biología Molecular y Celular, Facultad de Ciencias Exactas y Naturales (FCEN), Universidad de Buenos Aires (UBA) and Instituto de Fisiología, Biología Molecular y Neurociencias (IFIBYNE-UBA-CONICET), Ciudad Universitaria, Pabellón IFIBYNE (C1428EHA), Buenos Aires, Argentina, [2]Centro de Investigación en Bioquímica Clínica e Inmunología (CIBICI-CONICET) and Departamento de Bioquímica Clínica, Facultad de Ciencias Químicas, Universidad Nacional de Córdoba, Córdoba, Argentina, [3]Fondazione Istituto FIRC di Oncologia Molecolare (IFOM), Via Adamello 16, 20139 Milan, Italy and [4]Departamento de Biodiversidad y Biología Experimental, FCEN, UBA

Received February 03, 2020; Revised April 17, 2020; Editorial Decision April 20, 2020; Accepted April 23, 2020

ABSTRACT

We have previously found that UV-induced DNA damage causes hyperphosphorylation of the carboxy terminal domain (CTD) of RNA polymerase II (RNAPII), inhibition of transcriptional elongation and changes in alternative splicing (AS) due to kinetic coupling between transcription and splicing. In an unbiased search for protein kinases involved in the AS response to DNA damage, we have identified glycogen synthase kinase 3 (GSK-3) as an unforeseen participant. Unlike Cdk9 inhibition, GSK-3 inhibition only prevents CTD hyperphosphorylation triggered by UV but not basal phosphorylation. This effect is not due to differential degradation of the phospho-CTD isoforms and can be reproduced, at the AS level, by overexpression of a kinase-dead GSK-3 dominant negative mutant. GSK-3 inhibition abrogates both the reduction in RNAPII elongation and changes in AS elicited by UV. We show that GSK-3 phosphorylates the CTD *in vitro*, but preferentially when the substrate is previously phosphorylated, consistently with the requirement of a priming phosphorylation reported for GSK-3 efficacy. In line with a role for GSK-3 in the response to DNA damage, GSK-3 inhibition prevents UV-induced apoptosis. In summary, we uncover a novel role for a widely studied kinase in key steps of eukaryotic transcription and pre-mRNA processing.

INTRODUCTION

Gene expression is tightly regulated by external and internal cues. This includes gene expression activation and inhibition, *i.e.* regulation of transcription both at the initiation and elongation levels, as well as the generation of different mRNA variants. Co-transcriptional RNA processing events are greatly influenced by RNAPII transcription kinetics. In particular, alternative splicing (AS) decisions can be modulated by elongation rates, as explained by the kinetic model of coupling between transcription and AS: changes in the speed of elongation affect the time of emergence of nascent pre-mRNA, creating different windows of opportunity for the binding of positive and negative splicing factors to both splicing sites and splicing enhancers and silencers (1). This phenomenon can explain upregulation of both alternative exon cassette inclusion or skipping at low elongation rates, depending on the architecture of the nascent RNA and the nature of the splicing regulatory elements (2,3).

Rpb1, the largest subunit of RNAPII, has a distinctive feature: it has a long repetitive carboxy terminal domain (CTD) of the consensus heptapeptide YSPTSPS. The CTD is highly conserved among eukaryotes, with variation in its length. For instance, in yeast the CTD comprises 26 repeats, while in humans, 52. The CTD is largely modified by phosphorylation along gene transcription. According to a classic paradigm, CTD phosphorylation at Ser5 (P-Ser5) by Cdk7, the kinase subunit of TFIIH, is a hallmark of transcription initiation, while the transition from initiation to productive elongation is mediated by Ser2 phosphorylation by Cdk9, a component of the P-TEFb complex. Though instrumental to depict the transcription cycle, the real situation is much more complex due to, at least, three reasons. First, because of its repetitive nature, it is challenging to know the detailed phosphorylation pattern of the whole CTD. In this sense, a big effort was done by the Eick lab, who showed that there is a high variability of phospho- amino acid combinations within single and adjacent heptads, thus demonstrating the heterogeneity along the CTD (4). Second, as kinases and phosphatases modify the CTD along the gene body, the phosphorylation state of the CTD varies

*To whom correspondence should be addressed. Tel: +54 11 4576 3368; Email: ark@fbmc.fcen.uba.ar

pronouncedly. In fact, intragenic P-Ser5 signal was detected while transcribing alternative exons (5) and Proudfoot and Carmo-Fonseca's labs showed that, in particular, there are high peaks of P-Ser5 positioned at 5′ splice sites that coordinate splicing with transcription (6). Third, apart from the canonical Cdk7 and Cdk9 duet, there are other kinases that modify the CTD. Ser2 phosphorylations downstream into the gene body are catalyzed by Cdk12 and Cdk13 (7) and modulate RNA processing events (8). P-Thr4 marks are placed by Plk3 on RNAPII located towards the 3′ end of genes (9). The kinase Dyrk1A binds to the promoter of a subset of genes and promotes transcription by phosphorylating the CTD (10) and, in complex with DCAF7, is tethered to RNAPII and promotes myogenesis (11). The atypical kinase BRD4 was also shown to phosphorylate the CTD *in vitro* (12) and its activity is relevant for AS regulation during thymocyte differentiation (13). Finally, a recent screening of yeast kinases unveiled novel P-Thr4 CTD kinases, and that hrr25, the yeast homolog of CK1, regulates snoRNA maturation via phosphorylation of RNAPII at Thr4, thus supporting the concept of gene-class-specific CTD kinases (14).

UV-induced DNA damage triggers a transcriptional response that modifies transcription and AS patterns genome-wide in the context of the kinetic coupling model (15,16). This response consists of two parallel mechanisms. The in *cis* response starts with the encounter of a transcribing RNAPII with a DNA lesion which triggers transcription-coupled nucleotide excision repair pathway (TC-NER) (17–19). The in *trans* response that we study here is independent from TC-NER and consists of a signaling that begins with the repair of the UV-induced cyclobutane pyrimidine dimers (CPDs) by the global genome nucleotide excision repair pathway (GG-NER) and results in an extensive hyperphosphorylation of the RNAPII CTD, detected by western blot as an increase in RNAPII O isoform (hyperphosphorylated) with respect to RNAPII A (hypophosphorylated). In turn, this phosphorylation correlates with reduced transcription elongation rates that change AS patterns in the context of the kinetic coupling model. ATR, a paramount DNA damage response kinase, is involved in this signaling in skin cells, probably indirectly (20). Cdk9, as part of P-TEFb, is also involved. Evidence of this is that camptothecin or UV treatment induce the dissociation of P-TEFb from its inhibitory counterpart HEXIM/7SK and promote RNAPII CTD hyperphosphorylation (21,22). It is worth noting, however, that the treatment with Cdk9 inhibitors *per se* induces a complete switch in RNAPII western blot signal towards RNAPII A. Thus, though necessary to promote RNAPII hyperphosphorylation, Cdk9 may not be the only kinase involved.

Given this scenario, we were interested in finding new kinases participating in the transcriptional response to DNA damage. Therefore, we developed a screening strategy based on an AS fluorescent reporter that allowed us to test *ca.* 700 kinase inhibitors to identify those that reduce or abolish the AS response to UV-induced DNA damage. Glycogen synthase kinase 3 (GSK-3) emerged as the principal common target, so we centered our attention in understanding its role in this response. Here we show that GSK-3 inhibition prevents RNAPII hyperphosphorylation and changes in AS patterns and transcription elongation rates in response to UV irradiation. The inhibitory drug effect is not due to differential degradation of the phospho-CTD isoforms and can be reproduced, at the AS level, by overexpression of a kinase-dead GSK-3 dominant negative mutant, which supports an *in viv*o role for GSK-3 in the in *trans* pathway. *In vitro* experiments show that GSK-3 phosphorylates the CTD directly but preferentially when the substrate is previously phosphorylated by another kinase such as Cdk9, consistently with the requirement of a priming phosphorylation reported for GSK-3 (23). In line with a role for GSK-3 in the transcriptional response to DNA damage, GSK-3 inhibition prevents UV-induced apoptosis. In summary, data presented in this paper position GSK-3 as a novel CTD kinase responsible for the RNAPII hyperphosphorylation caused by DNA damage, thus assigning a novel role for this widely-studied kinase.

MATERIALS AND METHODS

Cell culture and treatments

HeLa and HEK293T cells were cultured as indicated by ATCC. HeLa Flp-In T-REx cells were gently provided by Matthias Hentze. HeLa Flp-In T-Rex cells were cultured in the presence of zeocin (Invitrogen) 100 μg/ml and blasticidin (Invivogen) 5 μg/ml. HeLa Flp-In T-REx stably transfected cells were cultured in the presence of hygromycin (Invivogen) 100 μg/ml and blasticidin 5 μg/ml. Tet-on promoters were induced by the addition of tetracycline (Sigma) 1 μg/ml. Endogenous RNAPII inhibition was achieved by the addition of α-amanitin (Sigma) 10 μg/ml. UV irradiation was performed as described previously (20). GW806290X and GW805758X (GlaxoSmithKline) were used at 0.1 and 0.5 μM respectively. Commercial GSK-3 inhibitors CHIR99021 and AR-A 014418 (Sigma) were used at 10 and 20 μM respectively. Cdk7/9 inhibitor DRB (Sigma) was used at 50 μM. Actinomycin D was used at 10 μg/ml. MG132 was used at 10 μM.

Transfections and stable cell lines

Transfections were performed using Lipofectamine 2000 (Thermo Scientific) according to the manufacturer's instructions. Flp-In T-REx stable cell lines were obtained by co-transfection of the gene of interest cloned in the plasmid pCDNA5/FRT/TO and the plasmid pOG44, according to the manufacturer's manual (Invitrogen). WT and K85A GSK-3β constructs were gently provided by Scott Friedman. For experiments where GSK-3β expression plasmids and AS reporter minigene plasmids were co-transfected, a ratio 9:1 of former to the latter plasmid was used in the transfection mix.

RNA extraction, RT-PCR, RT-qPCR and qPCR

RNA was purified using TriPure reagent (Roche Life Science). RT reactions were performed with MM-LV RT (Invitrogen) following the manufacturer's instructions using random decamers as primers. PCR and qPCR conditions and primers are described in the Supplemental Experimental Procedures.

Western blot

Protein samples were prepared in 2× Laemmli buffer. Western blot procedures and antibodies are detailed in the Supplemental Experimental Procedures.

Epifluorescence microscopy and data analysis

Cells growing in Lab-Tek II chambers (Thermo) were fixed by incubation with 4% PFA in PBS for 10 min and rinsed 3 times in PBS. Nuclei were stained by addition of DAPI 1 μg/ml in PBS. Images were obtained with an Olympus IX81 epifluorescence microscope and processed with the CellProfiler software (Broad Institute) to segment nuclei and quantify dsRed and GFP fluorescence signal. Data analysis was performed with RStudio software.

CPD removal by CPD photolyase

HeLa cells expressing the marsupial CPD photolyase of *Potorous tridactylus* were obtained via the Flp-In T-REx system by subcloning the photolyase used previously (20) in the plasmid pcDNA5/FRT/TO. Photolyase expression was induced by addition of tetracycline to the culture medium for 24 h prior to transfection with the fluorescent reporter. Immediately after irradiation, tetracycline was re-added to induce the fluorescent reporter and cells were exposed to white light to activate the photolyase-mediated CPD removal or kept in the dark as a control.

Kinase inhibitors screening and data analysis

The screening with PKIS2 (GlaxoSmithKline) kinase inhibitor library was divided in subsets. For each subset, 10 000 HeLa eRGi cells were plated in 96-well plates. Twenty-four hours later, cells were irradiated (or not) with 5 J/m^2 of UV light, and tetracycline and a different kinase inhibitor at 0.1 μM in each well (or DMSO as a vehicle control) were added immediately. Twenty-four hours later, cells were harvested by trypsinization and GFP and dsRed* fluorescence signal were acquired in a robot-assisted flow cytometer Attune NxT (Thermo). Prior to trypsinization, cells were observed at the microscope to detect any possible toxicity associated with the inhibitor treatment.

The data obtained with the flow cytometer were analyzed with RStudio software as follows: (i) mean GFP signal over mean dsRed signal (GFP signal)/(dsRed signal) was calculated for each well, both for the non-irradiated and the irradiated plates; (ii) for each plate, the average (GFP signal)/(dsRed signal) of the four vehicle control (DMSO) wells and its associated error were calculated and noted as $DMSO_{Ctrl} \pm s$ or $DMSO_{UV} \pm s$; (iii) the ratio of $DMSO_{UV}/DMSO_{Ctrl}$, defined as $Q_{DMSO} \pm s$, represents the average effect of UV treatment with vehicle; (iv) for each inhibitor, the ratio (GFP signal)/(dsRed signal) was calculated for non-irradiated and UV irradiated cells, noted as Inh_{Ctrl} and Inh_{UV} respectively. The ratio Inh_{UV}/Inh_{Ctrl} was noted as Q_{Inh}, and corresponds to the effect of UV treatment when cells are treated with the corresponding inhibitor; (v) inhibitors were considered positive hits when Q_{Inh} was greater or less than $Q_{DMSO} \pm 2s$ and the percentage of change was equal or more than 15%. Positive hits were repeated in an independent experiment to rule out false-positive hits.

In vitro kinase assays

GST-CTD constructs were expressed in *E. coli* and prepared as indicated previously (24). To prepare Cdk9, GSK-3β and HA-tagged WT and KD GSK-3β, HEK293T cells were lysed at 4°C for 30 min in IP buffer (20 mM HEPES pH 7.4, 1% Igepal, 150 mM NaCl, 10 mM KCl, 0.1 mM EGTA, 0.1 mM EDTA, 1 mM DTT, 1× PhosStop (Roche) phosphatase inhibitor cocktail and 1× cOmplete (Roche) protease inhibitor cocktail). Lysates were cleared by centrifugation at 12 000 g for 10 min and the indicated antibody was added to 1.6 mg of total protein and incubated with rotation at 4°C for 2 h. Aliquots of 30 μl of Dynabeads Protein G (Thermo) were equilibrated and added to the antibody:lysate suspensions and incubated with rotation at 4°C for two additional hours. Beads were rinsed twice with 500 μl of IP buffer and twice with 500 μl of kinase buffer (60 mM HEPES pH 7.4, 10 mM $MgCl_2$, 1 mM $MnCl_2$, 1.2 mM DTT, 1× PhosStop (Roche) phosphatase inhibitor cocktail and 1× cOmplete (Roche) protease inhibitor cocktail) and finally resuspended in 30 μl of kinase buffer. Kinase reactions were performed at 30°C by addition of 10 μl of kinase attached to the beads to 100 ng of GST-CTD in a final volume of 30 μl with ATP at 250 μM for Cdk9 reactions or at 1 mM for GSK-3 reactions. Rabbit normal IgG was used as a control for GSK-3 reactions. When added, CHIR99021 was used at 10 μM. Kinase immunoprecipitations were performed with anti Cdk9 (C-20, Santa Cruz), anti GSK-3β (27C10, Cell Signaling) and anti HA (H6908, Sigma).

Differential cell extract preparation

The differential salt extractability protocol used was described previously (21).

Chromatin immunoprecipitation

RNAPII ChIP experiments were performed as in (25) with Rpb1 NTD (D8L4Y) rabbit antibody (Cell Signaling).

Propidium iodide and FITC-annexin V staining

Apoptosis staining was performed with Annexin V-FITC Apoptosis detection kit (BD) following the manufacturer's instructions and analyzed in a FACS Aria II flow cytometer (BD).

Cloning, subcloning and reverse fluorescent reporter construction

The original version of the fluorescent alternative splicing reporter was a gentle gift of Thomas Cooper. The original reporter was subcloned in the plasmid pcDNA5/FRT/TO with the enzymes HindIII and ApaI. Mutagenesis of dsRed (H41T/N42Q/V44A) and the reverse reporter were obtained by traditional site-directed mutagenesis. Primers used are listed in the Supplemental Experimental Procedures.

Cloning of the TMEM188-E2 AS reporter minigene

TMEM188-E2 minigene was obtained by cloning a DNA fragment containing the alternative exon E2, its flanking introns, and part of the upstream and downstream exons into the BstEII sites of the TBX3-E2a minigene vector (20). The primers used for cloning are detailed in the Supplemental Experimental Procedures.

CRISPR/Cas9 mediated knock-out

GSK-3α and GSK-3β knock-out cells were obtained according to (26). gRNAs were designed targeting the sequences 5′-GACAGATGCCTTTCCGCCGCCGG-3′ for GSK-3α and 5′-CTTGCAGCTCTCCGCAAAGGAGG-3′ for GSK-3β.

RESULTS

An improved fluorescent reporter for alternative splicing

In order to identify new protein kinases involved in the transcriptional and AS response to UV-induced DNA damage, we decided to modify an AS fluorescent reporter developed by the Cooper lab (27). This reporter includes the 28-bp alternative cassette exon 5 of chicken troponin T (cTNT E5) whose exclusion determines the expression of the dsRed protein whereas its inclusion causes expression of GFP, with both fluorescent proteins being directed to the nucleus. This reporter is useful to study AS regulation changes in steady-state. However, since the response to UV-induced DNA damage is transient and UV treatment induces a strong shut-down of transcription and translation, some major changes were mandatory. First, we subcloned the reporter under the control of the inducible Tet-on promoter of the pcDNA5/FRT/TO plasmid that, additionally, allows direct integration into the genome of the transfected cells via the Flp-In T-Rex system (Invitrogen). Second, since the maturation half-time of dsRed is approximately 10 times longer than that of GFP (28), we introduced three mutations leading to amino acid changes (H41T, N42Q and V44A) reported to promote faster maturation (29). The final version of the construct with the fast maturating dsRed (dsRed*) is depicted in Figure 1A. We obtained HeLa cells stably transfected with this construct (HeLa eRGi cells). Supplementary Figure S1 shows that dsRed* and GFP fluorescence increase comparably after induction by tetracycline in HeLa cells stably transfected with the modified reporter, while cells transfected with an inducible version of the original reporter only display GFP fluorescence 22 h after induction, suggesting that the modified reporter would be more sensitive to detect changes in inclusion of the alternative exon upon external signals.

The next step was to validate the designed reporter to evaluate the AS response to UV-induced DNA damage. Indeed, UV irradiation of HeLa eRGi cells upregulates inclusion of the cTNT exon E5 both at the mRNA (Figure 1B) and protein (Figure 1C) levels. Importantly, flow cytometry analysis shows that the GFP/dsRed* fluorescence ratio increases proportionally to the UV dose in a linear fashion (Figure 1D). Images obtained by epifluorescence microscopy (Figure 1E) also confirm that dsRed* fluorescence decreases with UV irradiation compared to GFP signal.

As an important control to demonstrate that the observed changes in fluorescence ratios are not due to artifactual features of the fluorescent proteins of the reporter, we obtained HeLa cells stably transfected with a 'reverse' reporter in which exon inclusion causes dsRed* fluorescence while exclusion promotes GFP signal (Supplementary Figure S2A). Both mRNA analysis and flow cytometry (Supplementary Figure S2B) clearly show that the effects of UV irradiation are reproduced with the 'reverse' reporter.

A second important aspect to investigate is if the upregulation of cTNT E5 inclusion follows the kinetic coupling mechanism. We have previously shown that DNA lesions caused by UV trigger RNAPII hyperphosphorylation leading to slow transcriptional elongation rates which in turn affect AS decisions (15,20). Figure 1F shows that the increase in inclusion of cTNT E5 caused by UV is abolished when transcription is carried out by an RNAPII with a non-phosphorylatable CTD at serines 2 and 5 (15) (lanes 1–4). In turn, transcription by a slow mutant (hC4 mutant, R749H) of RNAPII increases cTNT E5 inclusion (lane 5), coherently with a kinetic regulation of the AS of this exon (3). Furthermore, removal of the cyclobutane pyrimidine dimers (CPDs), the most abundant DNA lesions caused by UV, by ectopic expression of a marsupial CPD-specific photolyase in HeLa cells (20) also reduces the UV effect on cTNT E5 inclusion (Figure 1G). Altogether, results in Figure 1, Supplementary Figures S1 and S2 support the use of the HeLa cell line stably transfected with the improved fluorescent reporter to identify new protein kinases participating in the UV effect on AS, based on its kinetic coupling with transcription.

GSK-3 inhibitors specifically reduce the UV effect on alternative splicing

To perform a screening of protein kinase inhibitors, HeLa cells stably transfected with the improved fluorescent reporter were plated in 96-well plates at ∼10 000 cells per well. Twenty-four hours later, the cells were exposed or not to UV irradiation at a dose of 5 J/m^2 and treated with 688 different ATP-competitive protein kinase inhibitors, present in the GlaxoSmithKline published kinase inhibitor set 2 (PKIS2) library, at a final concentration of 0.1 μM. The expression of the reporter was induced by addition of tetracycline and, 24 h later, cells were harvested by trypsinization and fluorescence was assessed in a robot-assisted flow cytometer (Supplementary Figure S3A). Supplementary Figure S3B shows a diagram of the screening analysis and data treatment. Screening results are shown in Supplementary Table S1. Surprisingly, only 8 inhibitors reduced the effect of UV light on cTNT E5 inclusion by at least 15% and five of these were reported to target glycogen synthase kinase 3 (GSK-3, Figure 2A). In order to validate the effects of GSK-3 inhibition we tested two of the inhibitors from the library (GW806290X and GW805758X) and two commercial GSK-3 inhibitors (CHIR90221 and AR-A 014418, Figure 2B) in the AS response to UV exposure (Figure 2C-E). Unlike GW806290X and GW805758X, the commercial inhibitors CHIR and AR-A are selective for GSK-3 and do not inhibit Cdks (30,31). Commercial inhibitor activity was validated by analysis of the phosphorylation of β-catenin

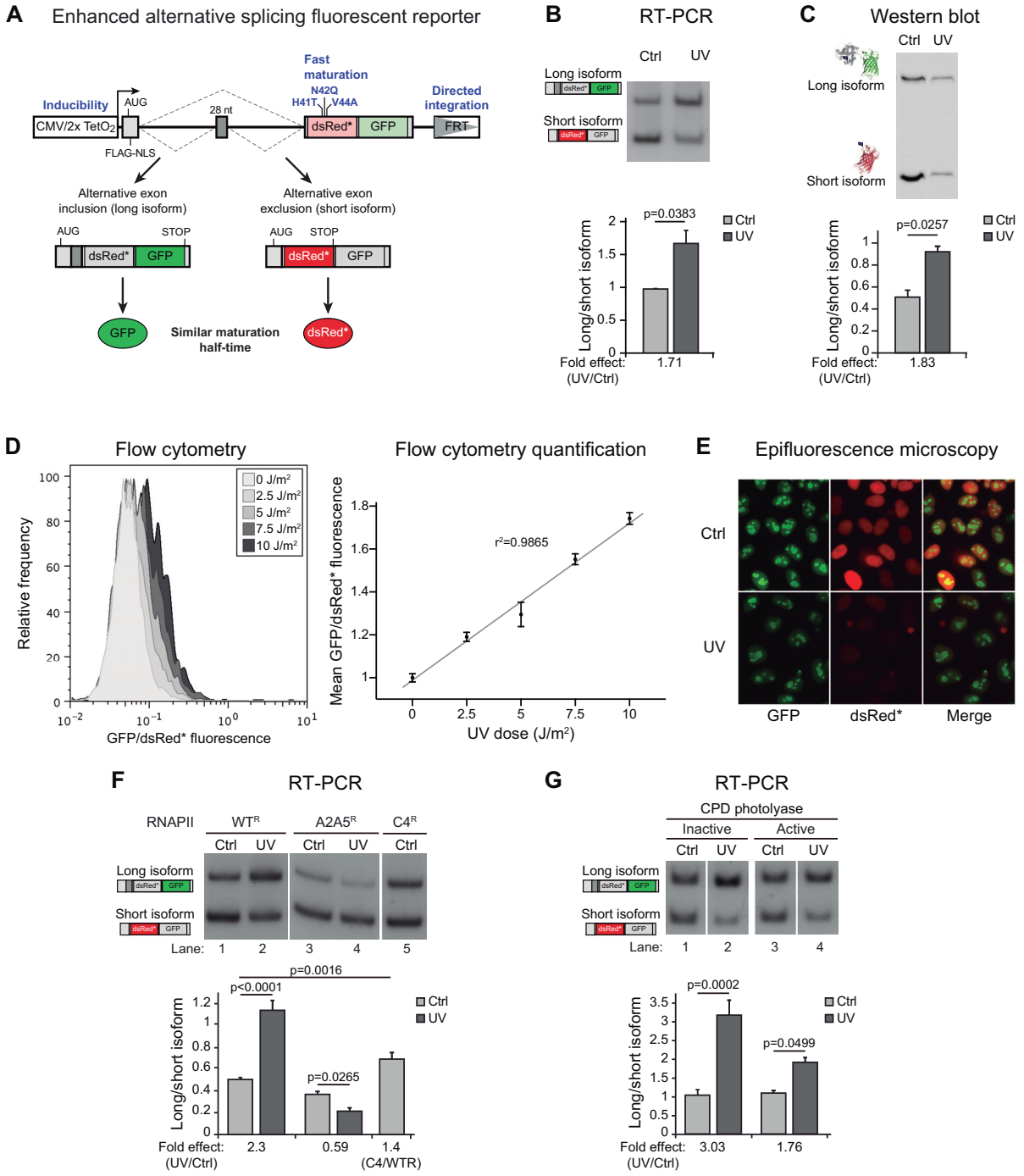

Figure 1. An alternative splicing fluorescent reporter system to study the transcriptional response to UV-induced DNA damage. (**A**) Diagram of the enhanced alternative splicing fluorescent reporter used to stably transfect HeLa cells by the Flp-In techonology (HeLa eRGi cells). Inclusion of the 28 nt alternative exon (cTNT E5) results in an mRNA that is translated to GFP, while the mRNA resulting from its skipping is translated to dsRed*. (**B**) HeLa eRGi cells were UV irradiated (or not) with 15 J/m^2 and tetracycline was immediately added to induce the transcription of the reporter. Three hours after irradiation, total RNA was prepared and AS patterns of the alternative splicing fluorescent minigene were assessed by radioactive RT-PCR with specific primers. The ratio inclusion/skipping is shown. (**C**) Western blot of the reporter-encoded proteins was performed with an anti-Flag antibody. HeLa eRGi cells were treated as in (B) and harvested in Laemmli buffer 24 hours after irradiation. (**D**) Flow cytometry of HeLa eRGi cells treated as in (B), with different doses of UV light, 24 h after irradiation. The left panel is a histogram of GFP/dsRed* fluorescence signal at each UV dose. The right panel shows the quantification of the mean GFP/dsRed* signal of 3 independent experiments. The r^2 of the linear regression is shown. (**E**) Epifluorescence microscopy representative fields of HeLa eRGi cells treated as in (B), 24 hours after irradiation. The figure shows GFP signal, dsRed* signal and their merge. (**F**) HeLa eRGi cells were transfected with WT, A2A5 and C4 α-amanitin resistant Rpb1 expression constructs. Twenty-four hours after transfection, α-amanitin was added at 100 μg/ml to induce the degradation of the endogenous Rpb1. Twenty-four hours later, cells were treated as in (B). Three hours after irradiation, total RNA was prepared and AS patterns were assessed by radioactive RT-PCR. (**G**) HeLa cells stably expressing the marsupial CPD photolyase were transfected with the alternative splicing fluorescent reporter construct shown in (A). Cells were treated as in (B) followed by 2 h under white light (or not as a control) to induce the repair of the CPDs. Three hours after irradiation, total RNA was prepared and AS patterns were assessed by radioactive RT-PCR.

A Screening results

Inhibitor	Putative target	% inhibition at 0.1 μM
GW806290X	**GSK-3β**, Cdk2, Cdk4	22%
GW801372X	**GSK-3β**, Cdk2, Cdk4	33%
GW779439X	**GSK-3β**, Cdk2, Cdk4	21%
GW493036X	Unknown	18%
GW872411X	ALK5	15%
SB-707548-A	Unknown	22%
GW810578X	**GSK3**	26%
GW805758X	**GSK-3β**, Cdk2, Cdk4	36%

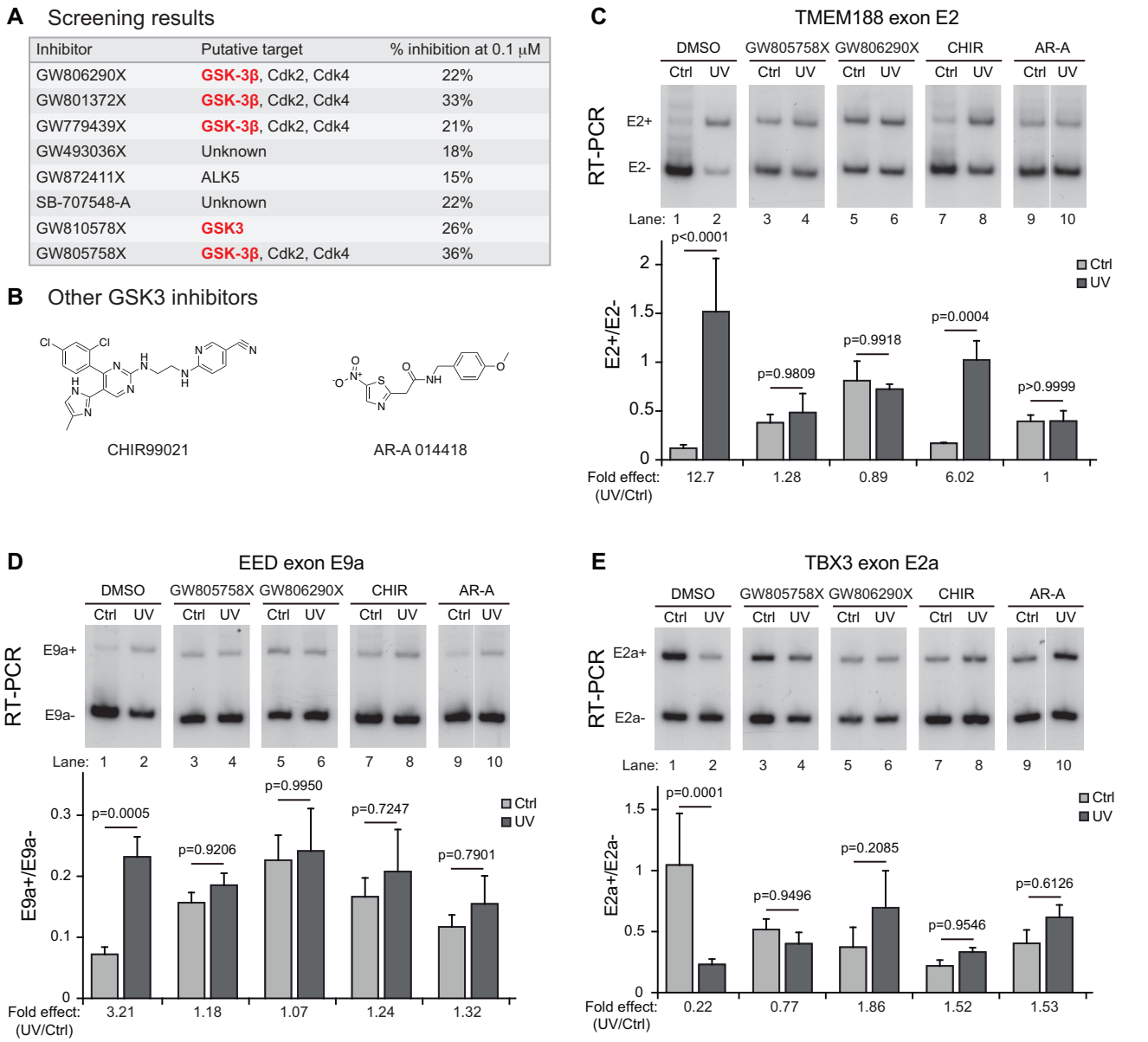

Figure 2. Screening of protein kinase inhibitors unveils GSK-3 as a kinase involved in the transcriptional response to UV-induced DNA damage (**A**) Hits resulting from the screening of the PKIS2 library with the alternative splicing fluorescent reporter. (**B**) Structure of the commercial selective GSK-3 inhibitors used. (C–E) HeLa cells were UV irradiated (or not) with 15 J/m^2 and the inhibitors GW8057578X, GW806290, CHIR, AR-A or DMSO as vehicle control were added immediately. Three hours after irradiation, total RNA was prepared and AS patterns of the alternative exons E2 of TMEM188 (**C**), E9a of EED (**D**) and E2a of TBX3 (**E**) were assessed by radioactive RT-PCR with specific primers.

at Ser33, Ser37 and Thr41, and of Tau at Ser396 (Supplementary Figure S3C), two well-known GSK-3 substrates (23). Inclusion of TMEM188 E2 is promoted by UV irradiation (Figure 2C, lanes 1 and 2) and this effect is abolished (lanes 3–6, 9 and 10) or reduced (lanes 7 and 8) by GSK-3 inhibitors. In the case of EED E9, where UV light also increases exon inclusion (Figure 2D, lanes 1 and 2), the four inhibitors abolish the UV effect (lanes 3–10) but they display an effect *per se* in promoting EED E9 inclusion. Unlike the two previous events, TBX3 E2a corresponds to an event in which UV light and slow elongation promote exon skipping (20). This downregulatory effect (Figure 2E, lanes 1 and 2) is also abolished by the four tested inhibitors (lanes 3–10), which display a *per se* effect similar to that of UV irradiation. It is worth noting that GSK-3 inhibition *per se* modifies AS patterns in non-irradiated cells. There are several possible explanations for this. This effect can be coupled to transcription if GSK-3 acts as an RNAPII kinase. It can also be a consequence of changes in splicing factor activities. This would not be surprising given that GSK-3 phosphorylates several splicing factors (32). Finally, it can be due to changes in mRNA isoforms stability, and thus not dependent on *de novo* transcription. The latter hypothesis was overruled. As shown before (15), the UV effect on AS is abolished by treatment of the cells with the transcription inhibitor actinomycin D. Consistently, in the presence of acti-

nomycin D, the GSK-3 inhibitor CHIR has no further effects *per se* or in the UV-treated cells on the three model AS events assessed in Figure 2 (Supplementary Figure S4A–C).

GSK-3 is an RNAPII phospho-CTD kinase

The inhibition of the UV effect on AS by GSK-3 inhibitors suggests that GSK-3 may be involved directly or indirectly in the phosphorylation of RNAPII. As a first approach we tested the effects of the four GSK-3 inhibitors in RNAPII western blot (Figure 3A). Notably, whereas the Cdk9 inhibitor DRB completely prevents RNAPII phosphorylation, both in irradiated and non-irradiated cells (lanes 11–14), GSK-3 inhibition only prevents RNAPII hyperphosphorylation caused by UV irradiation (lanes 1–10). This suggests that GSK-3 might be acting on pre-phosphorylated CTD (see below). Given that RNAPII is phosphorylated when engaged in transcription, we prepared differential cell extracts based on a salt extractability protocol (21). This protocol allows to obtain a high salt extract, which is enriched in transcribing RNAPII, and a low salt extract. Supplementary Figure S4D shows that, although RNAPII is present in both types of extract, UV-induced RNAPII hyperphosphorylation is observed in the high salt extract but not in the low salt extract (compare lanes 1 and 2 versus lanes 5 and 6). However, if cells are treated with the GSK-3 inhibitor CHIR, RNAPII hyperphosphorylation in response to UV is impaired (compare lanes 2 and 4).

Figure 3A also reveals that UV irradiation induces an observable decrease in total RNAPII western blot signal, no matter what inhibitor is used. This decrease is caused by proteasome-mediated RNAPII degradation (33). This opens the possibility that the effects of the GSK-3 inhibitors themselves were due to differential promotion or inhibition of the degradation of specific RNAPII isoforms. Figure 3B shows that pre-treatment with the proteasome inhibitor MG132 abolishes the observed degradation by UV and, most importantly, does not affect the abrogation of the UV effect by GSK-3 inhibition.

Given that the CTD repeats match the GSK-3 target consensus site (Figure 3C), we performed *in vitro* phosphorylation assays of recombinant CTD expressed in bacteria by the Cdk9 and/or GSK-3β endogenous kinases, immunopurified from HEK293T cells. Figure 3D shows that Cdk9 is able to phosphorylate the recombinant CTD with preference towards Ser5 over Ser2 (lane 3), as previously reported (34). In fact, if Cdk9 is incubated with the CTD for shorter times, no P-Ser2 signal is detected (lane 4). Figure 3E shows that immunopurified GSK-3β can phosphorylate the CTD at Ser2 to some extent (lane 3). However, when recombinant CTD is pre-phosphorylated by Cdk9 (P-CTD), GSK-3β phosphorylation efficiency increases by at least 5-fold (compare lanes 3 and 5). Moreover, GSK-3β is also able to phosphorylate Ser5 of a CTD pre-phosphorylated by Cdk9 (Supplementary Figure S5A). To rule out that the immunopurified preparation of GSK-3β contained contaminating kinases other than GSK-3β that could be responsible for the phosphorylation of phospho-CTD, we expressed HA-tagged WT GSK-3β and the kinase-dead (KD) mutant K85A (35) in HEK293T cells and immunopurified them with an anti-HA antibody. Unlike WT HA-GSK-3β, the KD mutant is not able to phosphorylate the recombinant CTD pre-phosphorylated by Cdk9 neither at Ser2 (Figure 3F) nor at Ser5 (Supplementary Figure S5B). These experiments reveal that, consistently with the requirements to phosphorylate its canonical substrates like β-catenin and Tau (23), GSK-3 efficiently acts as a CTD kinase when the CTD is already phosphorylated. In summary, our results suggest that GSK-3 phosphorylates phospho-CTD in a direct manner.

Redundancy and requirement of GSK-3α and GSK-3β

The two paralogue genes GSK-3α and GSK-3β share an 85% of amino acid sequence identity that increases to >95% at the catalytic domain. Although the two forms differ by the presence of an extra glycine-rich segment in GSK-3α, there is evidence that they might be redundant in the phosphorylation of certain targets (36). To investigate this possibility, we obtained CRISPR/Cas 9 knockouts of either GSK-3α or β in HeLa cells (Supplementary Figure S5C). After several attempts, we failed to obtain the double knockout in these cells which suggests that the complete absence of GSK-3 activity is not compatible with HeLa cell viability. The apparent essentiality of GSK-3 is not surprising, considering that ESCs differentiation is impaired in GSK-3 double KO cells (36). In any case, individual ablation of GSK-3α or GSK-3β did not prevent the UV effect on AS (Supplementary Figure S5D) nor on RNAPII hyperphosphorylation (Supplementary Figure S5E), indicating that the two GSK-3 forms play similar roles in the mechanism studied here and are therefore redundant. However, when GSK-3β was silenced using siRNA in the GSK-3α knockout cells, we were able to detect up to a 40% reduction in RNAPII hyperphosphorylation in response to UV irradiation. Conscious that still this evidence is not sufficiently strong, we explored another approach to validate the results with pharmacological inhibitors.

Overexpression of a kinase-dead dominant negative GSK-3β mutant reduces the UV effect on alternative splicing

In search for stronger genetic evidence to independently validate the results observed with the GSK-3 inhibitors we overexpressed the kinase-dead (KD) K85A GSK-3β mutant described above (Figure 3B). This mutant version of GSK-3β competes with endogenous active GSK-3 when expressed in cells, and thus acts in a dominant negative manner (37). Limitations of this approach due to low transfection efficiency were overcome by co-transfecting the GSK-3β expression plasmids with inducible AS reporter minigenes that contain intronic and exonic elements of an endogenous AS event under the control of a tetracycline inducible promoter. Furthermore, in order to avoid competition between endogenous GSK-3α and the GSK-3β overexpressed, these experiments were performed in GSK-3α null HeLa cells. As these cells derive from the HeLa Flp-In T-REx cells, they stably express the tetracycline repressor.

In brief, GSK-3α null cells were co-transfected with HA-tagged K85A GSK-3β mutant (or GSK-3β WT as a control) together with a TBX3 exon E2a AS reporter minigene (TBX3-E2a minigene, 20) or a TMEM188 exon E2

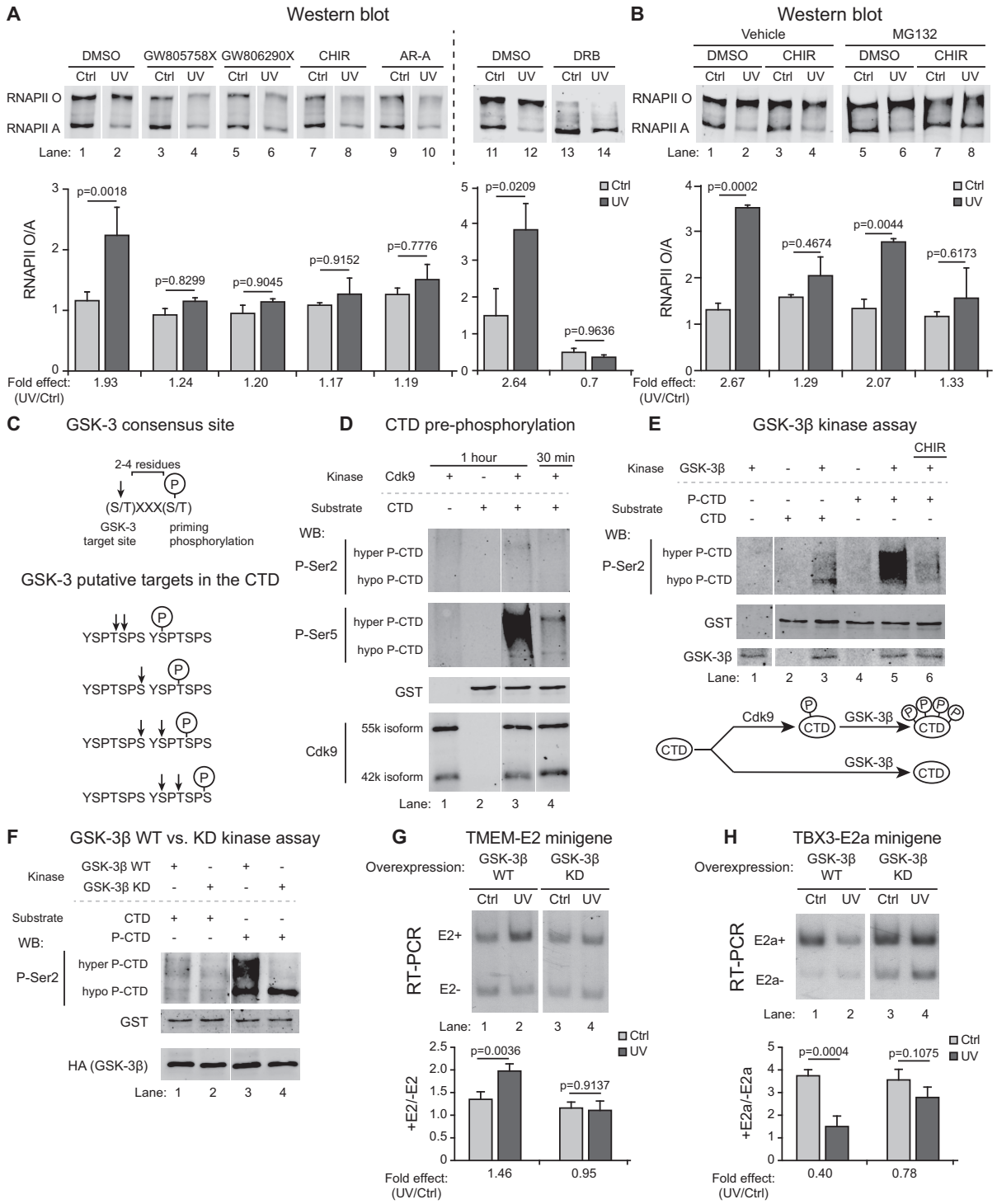

Figure 3. GSK-3 is an RNAPII phospho-CTD kinase and its activity is necessary for RNAPII hyperphosphorylation and AS response after UV-induced DNA damage (**A**) HeLa cells were UV irradiated (or not) with 15 J/m^2 and the inhibitors GW8057578X, GW806290, CHIR, AR-A or DMSO as vehicle control were added immediately. For DRB treatment, cells were pretreated for 2 h with DRB before UV irradiation. Two hours after irradiation, cells were harvested in Laemmli buffer and RNAPII phosphorylation patterns were assessed by western blot of total Rpb1. (**B**) HeLa cells were pre-treated (or not) with the proteasome inhibitor MG132 for 1 hour prior to irradiation. Subsequent treatment and sample analysis were performed as in (A). (**C**) Diagram of GSK-3 consensus site and putative GSK-3 target sites in a diheptad of the RNAPII CTD depending on which residue is previously phosphorylated. (**D**) Recombinant GST-CTD purified from bacteria was incubated with Cdk9 immunopurified from HEK293T cells in the presence of ATP. Cdk9 with no substrate and GST-CTD with no kinase were incubated in the presence of ATP as a control. After thirty minutes (or one hour), kinase assays were stopped by addition of Laemmli buffer and samples were analyzed by western blot with antibodies raised against CTD P-Ser2, CTD P-Ser5, GST and Cdk9. (**E**) GSK-3β was immunopurified from HEK293T cells. The kinase was incubated in the presence of ATP with GST-CTD purified from bacteria or with GST-CTD pre-phosphorylated (P-CTD) by Cdk9 as in (C). GSK-3 with no substrate was incubated in the presence of ATP as a control. Additionally, GSK-3 was incubated with (P-CTD) in the presence of ATP and CHIR. After one hour, kinase assays were stopped by addition of Laemmli buffer and

AS reporter minigene (TMEM188-E2 minigene). Twenty-four hours after transfection, cells were irradiated or not with 15 J/m^2 of UV light and tetracycline was immediately added to induce the AS reporter expression. Three hours later, cells were harvested for total RNA purification and analysis of minigene AS patterns were performed by radioactive RT-PCR with specific primers. Figure 3G (lanes 1 and 2) shows that UV irradiation causes an increase in TMEM188-E2 minigene exon E2 inclusion when cells overexpress GSK-3β WT, consistent with what happens with the endogenous TMEM188 exon E2 event (Figure 2C, lanes 1 and 2). However, upon overexpression of the KD dominant negative mutant (Figure 3G, lanes 3 and 4), there is no UV-effect on TMEM188-E2 minigene AS. Similarly, UV-irradiation increases TBX3-E2a minigene exon E2a skipping in cells overexpressing GSK-3β WT (Figure 3H, lanes 1 and 2) while overexpression of the KD dominant negative GSK-3β leads to an important reduction in UV-elicited exon E2a skipping (Figure 3H, lanes 3 and 4). In summary, these results reveal that the effect of GSK-3 pharmacological inhibitors on AS regulation in response to UV irradiation is reproduced if GSK-3 activity is inhibited competitively by the overexpression of a KD dominant negative mutant of GSK-3β.

RNAPII densities and histone 3′end processing are affected by GSK-3 inhibition

It is now accepted that UV irradiation causes a global reduction not only in RNAPII transcription initiation but also in elongation rates and that this effect is in *trans* and independent of the impairments to RNAPII progression caused in *cis* by the actual DNA lesions (15,16,20). Consequently, RNAPII ChIP experiments should reveal a relative decrease in promoter signal and an increase in intragenic signal upon UV treatment. We therefore decided to test if GSK3 inhibition affected RNAPII densities on the model gene *TBX3* by total RNAPII ChIP (Figure 4A). In fact, UV irradiation causes an important increase in RNAPII densities along the whole *TBX3* gene, except at its promoter region where the ChIP signal decreases. Such accumulation of RNAPII in the gene body is abolished when UV irradiated cells are treated with the GSK-3 inhibitor CHIR.

The Bentley lab has recently shown that inhibition of transcription elongation either by a slow mutant of RNAPII or by UV irradiation causes a change in 3′ end processing of the mRNAs encoding replicative histones (38). In normal conditions, the 3′ end of these mRNAs consists in a particular stem-loop structure. Slow elongation disrupts the formation of the stem–loop structure, which switches 3′ end formation to cleavage and polyadenylation occurring farther downstream. Therefore, slow elongation increases the ratio between the long histone mRNAs, resulting from cleavage and polyadenylation, over the short forms, resulting from stem–loop cleavage. This ratio could be used as a proxy to evaluate RNAPII elongation. Accordingly, we confirmed that UV irradiation increases the formation of the long mRNA for both histones H3B and H2AG and, most importantly, that these effects are greatly reduced by removal of the UV photolesions with the CPD photolyase approach used in Figure 1G (Figure 4B). As expected from the roles found here for GSK3 on AS and RNAPII phosphorylation, CHIR and AR-A inhibit the UV effect on promoting the longer mRNA isoforms of histones H3B and H2AG (Figure 4C). Summarizing, results in Figure 4 suggest that GSK3 inhibition counteracts the inhibition of RNAPII elongation triggered by UV-mediated DNA damage.

GSK3 inhibition reverts pro-apoptotic effects of UV irradiation

In an attempt to assess the biological implications of the role of GSK-3 in the UV-induced DNA damage response, we quantified the proportions of live, early apoptotic, late apoptotic and necrotic cells by flow cytometry using propidium iodide and FITC-annexin V. Upon UV irradiation, more than 95% of the cells are early or late apoptotic (compare Figure 5A and B). While CHIR has no effect on apoptosis *per se* (Figure 5C), it downregulates the UV effect on apoptosis by increasing the number of live cells from 3.8% to 51% and concomitantly reducing the proportion of early and late apoptotic cells to 45% (Figure 5D).

DISCUSSION

Our group has initially shown that UV treatment triggers a transcriptional and AS response that includes RNAPII hyperphosphorylation, a decrease in RNAPII elongation rates and genome-wide changes in AS patterns (15). Later, we found that the repair of CPD DNA lesions by the global genome nucleotide excision repair (GG-NER) machinery triggered a signaling cascade ending in RNAPII phosphorylation, mediated by the DNA damage kinase ATR (20).

Development of a fluorescent AS reporter system

In this work, our focus was to identify novel kinases involved in transcription and AS responses. To achieve this goal, we developed a screening strategy based on the AS fluorescent reporter originally designed by the Cooper lab (27). The original construction is useful to study stimuli that affect AS in the steady-state, but not for transient responses

←

samples were analyzed by western blot with antibodies raised against CTD P-Ser2, GST and GSK-3β. The diagram below depicts the experiment outcome. (**F**) HA-tagged WT or kinase dead (KD) GSK-3β were transfected in HEK293T cells and immunopurified with anti HA antibody. GST-CTD purified from bacteria or P-CTD were incubated with WT GSK-3β or KD GSK-3β in the presence of ATP. After one hour, kinase assays were stopped by addition of Laemmli buffer and samples were analyzed by western blot with antibodies raised against CTD P-Ser2, GST and HA. (**G**) HeLa GSK-3α null cells were co-transfected with WT GSK-3β (GSK-3β WT) or the kinase-dead dominant negative K85A GSK-3β mutant (GSK-3β KD) and a TMEM188 exon E2 AS reporter minigene. Cells were UV irradiated (or not) with 15 J/m^2 and tetracycline was added immediately to induce the AS reporter. Three hours after irradiation, total RNA was prepared and AS patterns of the minigene were assessed by radioactive RT-PCR with specific primers. (**H**) HeLa GSK-3α null cells were treated as in G, but in this case co-transfecting a TBX3 E2a AS reporter minigene.

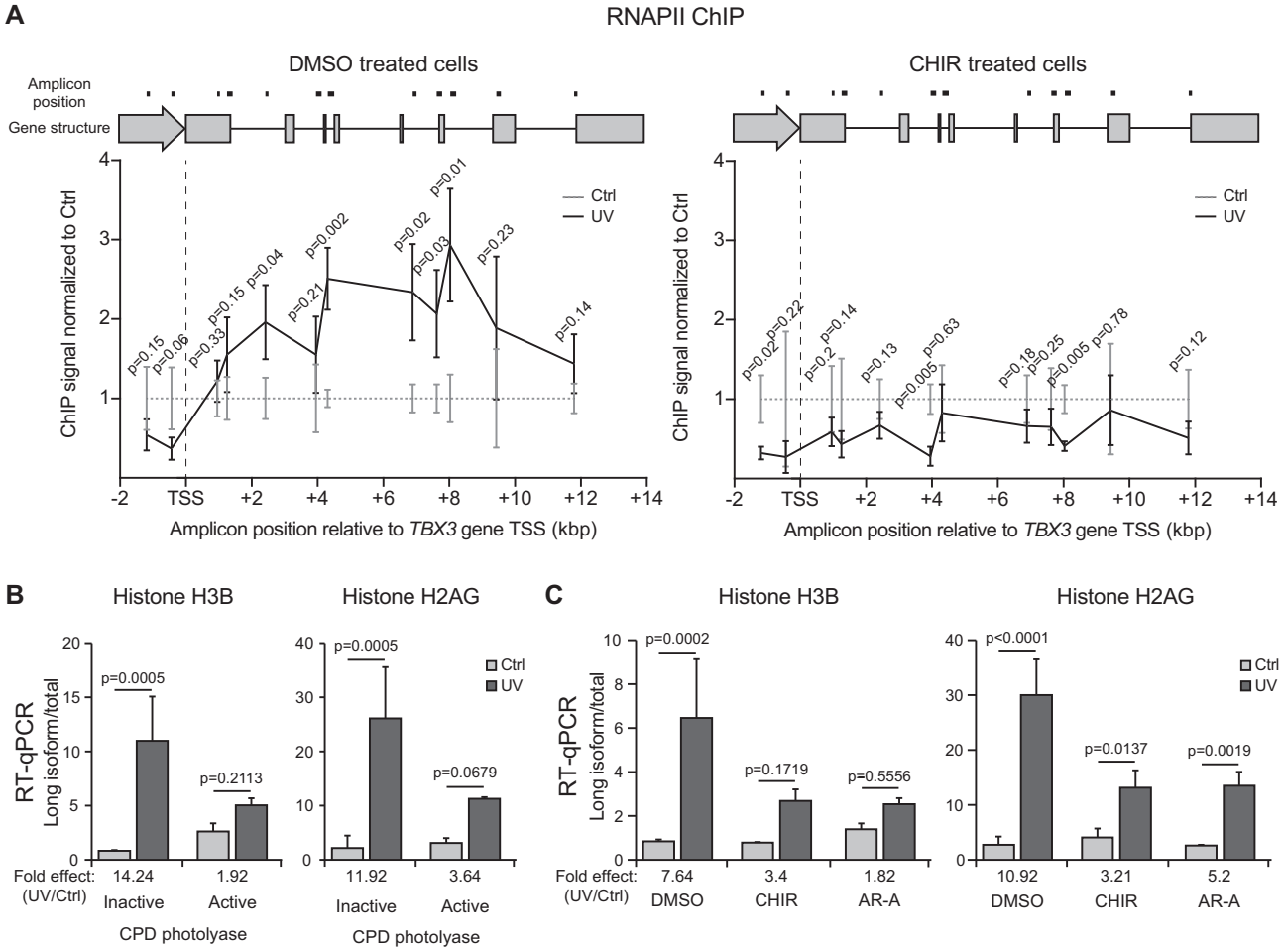

Figure 4. GSK-3 inhibition prevents the UV-induced reduction in RNAPII elongation rates (**A**) HeLa cells were UV irradiated (or not) with 15 J/m^2 and the inhibitor CHIR or DMSO as vehicle control were added immediately. Two hours later, cells were harvested for RNAPII ChIP. RNAPII density was measured along the *TBX3* model gene with the amplicons shown in the diagram. (**B**) HeLa cells stably transfected with the marsupial CPDs photolyase were UV irradiated (or not) and incubated 2 h exposed to white light (or not) to activate the CPD photolyases. Three hours after irradiation, total RNA was prepared and the quantity of long and total mRNA isoforms of histones H3B and H2AG were determined by RT-qPCR. The ratio long/total isoform is shown. (**C**) Quantification of histone H3B and histone H2AG long/total mRNA isoforms in response to UV-induced DNA damage in cells treated or not with the inhibitors CHIR and AR-A, three hours after irradiation.

like the one studied here. Therefore, we subcloned the reporter under a Tet-on promoter in a plasmid that allowed us to obtain a HeLa stable cell line via the Flp-In T-Rex system. Additionally, we introduced three point mutations in the dsRed coding sequence in order to obtain a fast maturing dsRed version (dsRed*), with a maturation half-time comparable to that of GFP. This enhanced reporter proved to be a useful tool to study UV induced changes in transcription and AS (Figure 1).

Screening reveals GSK-3 as a central kinase in the transcriptional and AS response to DNA damage

The optimized reporter was then used to screen the GlaxoSmithKline published kinase inhibitor set 2 (PKIS2) library, composed of nearly 700 different ATP-competitive protein kinase inhibitors. From the eight compounds that reduced the AS response to UV treatment, five had GSK-3 as a common target (Figure 2A). Therefore, we centered our attention on understanding the role of this kinase in the transcriptional and AS response to UV-induced DNA damage. The role of GSK-3 was further validated with the highly selective GSK-3 inhibitors CHIR99021 and AR-A 014418 (Figure 2B). It is important to note that, regarding the inherent pleiotropic nature of ATP-competitive kinase inhibitors, the use of different inhibitors is necessary to confirm the identity of the intervening kinase. In this sense, *in vitro* kinase assay screenings with CHIR99021 and AR-A 014418 showed that while both drugs inhibit efficiently the paralogues GSK-3α and GSK-3β, their off-target kinases are different (39).

GSK-3 phosphorylates the RNAPII CTD and affects elongation rates and AS patterns in response to DNA damage

We observed that GSK-3 inhibition prevents the transcriptional and AS response to UV-induced DNA damage at every level. First, GSK-3 inhibition prevents changes in AS patterns (Figure 2C–E), and this was also observed when, instead of using pharmacological inhibitors of GSK-3, we

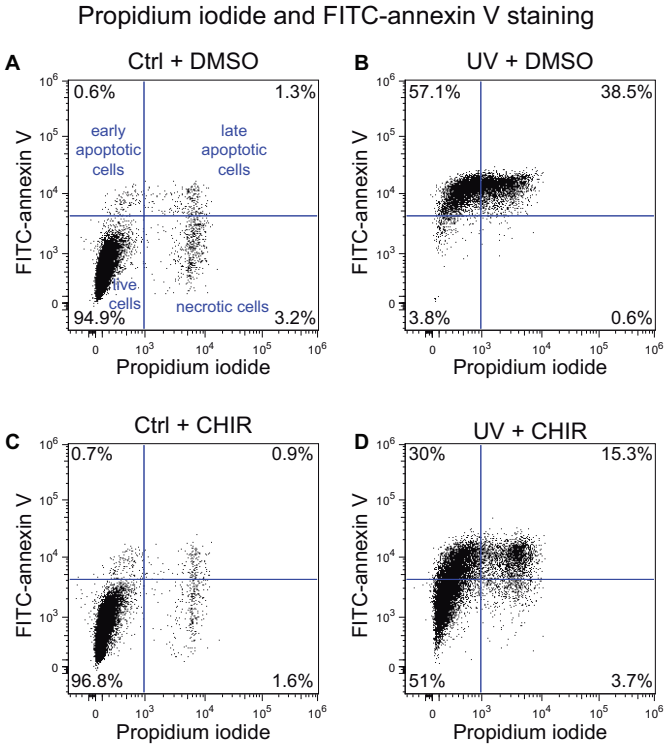

Figure 5. GSK-3 inhibition prevents UV-induced apoptosis (**A**–**D**) HeLa cells were UV irradiated with 30 J/m^2 to induce apoptosis, and immediately treated (or not) with CHIR. Twenty-four hours after UV irradiation, cells were stained with propidium iodide and FITC-annexin V to identify live, early apoptotic, late apoptotic and necrotic cells.

overexpressed a kinase-dead dominant negative mutant of GSK-3β (Figure 3G–H). It is fair to point out that, in some cases, GSK-3 inhibition modifies AS patterns *per se*. This is highly coherent with the role assigned here for GSK-3 as an RNAPII CTD kinase, and in fact, genome-wide analyses reveal that GSK-3 inhibition changes AS patterns globally (40). In this sense, there is a possibility for GSK-3 to have a role in transcription elongation in non-irradiated conditions and thus its inhibition would induce changes in AS regulation. Additionally, the change in AS patterns upon treatment with GSK-3 inhibitors could be a consequence of changes in splicing factor activities, since many of them are phosphorylated by GSK-3 (32). Though this hypothesis is plausible, its testing is beyond the scope of this work. Second, while Cdk9 inhibition prevents general RNAPII phosphorylation, GSK-3 inhibition seems to prevent only UV-induced RNAPII hyperphosphorylation. The relevance of GSK-3 in this specific situation may be the reason why, up to now, this activity has been out of sight (Figure 3A). Considering that the CTD sequence matches the GSK-3 target consensus site (41), we speculated that RNAPII could be a direct substrate of GSK-3 (Figure 3C). To test this hypothesis, we purified a GST-CTD fusion protein expressed in bacteria and immunopurified GSK-3β from HEK293T cells. When incubated together in *in vitro* phosphorylation conditions, GSK-3β phosphorylated the CTD mildly. However, if the CTD was subjected to a first round of phosphorylation by Cdk9, then GSK-3β was able to phosphorylate efficiently this pre-phosphorylated CTD (Figure 3D-F and Supplementary Figure S5A–B) both at Ser2 and Ser5. This is not surprising, considering that GSK-3 requires a priming phosphate around four residues C-terminal from the GSK-3 target amino acid to properly accommodate the substrate in its active site. In fact, GSK-3 yeast homologue Rim11 was shown to phosphorylate the CTD in Thr4 *in vitro,* but its biological relevance was not assessed (14). Third and last, GSK-3 inhibition prevents changes in elongation rates in response to DNA damage. This was shown with two different strategies: RNAPII densities were measured by ChIP experiments in cells treated or not with UV light, and treated or not with CHIR. UV treatment induces a relative decrease in RNAPII ChIP signal in the promoter and an increase in the gene body of the model gene *TBX3*. In turn, GSK-3 inhibition prevents the increase of the intragenic ChIP signal in response to UV treatment (Figure 4A). Alternatively, we measured histone mRNA polyadenylation as a proxy to evaluate RNAPII elongation rates: slow elongation induces a switch from the short stem-loop cleaved isoforms towards the long polyadenylated isoforms. This happens when cells are treated with UV light, but in combination with CHIR this switch is highly prevented (Figure 4C). Moreover, genetic evidence suggests that both paralogues GSK-3α and GSK-3β are redundant in this pathway (Supplementary Figure S5C-E). Altogether, our results suggest an important and direct role for GSK-3 in the UV-induced RNAPII hyperphosphorylation and the consequent changes in gene expression and AS patterns. However, the priming kinase(s) that phosphorylate(s) RNAPII prior to GSK-3 remain(s) unidentified. While Cdk9 is an obvious candidate (21,22), we cannot rule out if other kinase(s) may be involved.

Inhibition of RNAPII hyperphosphorylation versus degradation

We show here that, unlike DRB, GSK-3 inhibitors do not inhibit basal RNAPII phosphorylation but do inhibit UV-triggered CTD hyperphosphorylation (Figure 3A). Furthermore, both the UV-triggered hyperphosphorylation and its abrogation by GSK-3 inhibition are also observed when the proteasome activity is inhibited by MG132. This evidence is highly consistent with the in *trans* mechanism whose initial step is recognition of the DNA lesions by the GG-NER complexes and does not involve recognition of the lesion by RNAPII itself, followed by ubiquitylation and subsequent proteasomal degradation, as is characteristic of TC-NER.

GSK-3 collaborates in UV-induced apoptosis

There is compelling evidence that supports a role for GSK-3 in apoptosis. Intriguingly, while in the extrinsic apoptosis pathway GSK-3 acts as an anti-apoptotic factor, in the intrinsic pathway GSK-3 promotes apoptosis (42,43). UV-induced DNA damage triggers the intrinsic apoptosis pathway, that includes changes in gene expression profiles and is characterized by the release of cytochrome c from mitochondria that together with APAF-1 and procaspase-9 form the apoptosome. Apoptotic cells undergo a massive destabilization of cell structure that ends in cell death. GSK-3

was reported to promote apoptosis by phosphorylating key transcription factors, proteins that contribute to mitochondria disruption and proteins that destabilize the cytoskeleton, among others. These roles of GSK-3 were shown upon cell treatment with UV, camptothecin and etoposide (44–47). In Figure 5, we show that, as reported, GSK-3 inhibition prevents UV-induced apoptosis. However, the novelty of the present work resides on GSK-3 regulating gene expression profiles, including AS patterns, by directly modifying RNAPII elongation rates. The central role of GSK-3 in cell functioning is supported by evidence that its misregulation has been implicated in multiple pathologies including diabetes, cancer, bipolar disorder, cardiac disease and neurodegenerative conditions such as Alzheimer and Parkinson (48,49). Our demonstration that GSK-3 is an RNAPII phospho-CTD kinase and that its activity contributes to the modulation of RNAPII elongation opens the way to investigate if these mechanisms are implicated in the above-mentioned pathologies.

SUPPLEMENTARY DATA

Supplementary Data are available at NAR Online.

ACKNOWLEDGEMENTS

We thank V. Buggiano and A. Srebrow for their help and support. We also thank Isro Gloger and Kevin Madauss for providing the PKIS2 library from GSK. G.S., M.J.M., L.E.G. and A.R.K. are career investigators and N.N.M. and F.V. are recipients of postdoctoral and doctoral fellowships respectively from the Consejo Nacional de Investigaciones Científicas y Técnicas of Argentina (CONICET). C.C received an undergraduate fellowship from UBA.

FUNDING

A.R.K. and M.J.M received support from the Agencia Nacional de Promoción de Ciencia y Tecnología of Argentina [PICT 2014-2582]; Universidad de Buenos Aires (UBA); Lounsbery Foundation. G.S. received funding from the Agencia Nacional de Promoción de Ciencia y Tecnología of Argentina and GlaxoSmithKline [PAE-Glaxo 2014-0005].
Conflict of interest statement. None declared.

REFERENCES

1. Kornblihtt,A.R., Schor,I.E., Alló,M., Dujardin,G., Petrillo,E. and Muñoz,M.J. (2013) Alternative splicing: A pivotal step between eukaryotic transcription and translation. *Nat. Rev. Mol. Cell Biol.*, **14**, 153–165.
2. Dujardin,G., Lafaille,C., de la Mata,M., Marasco,L.E., Muñoz,M.J., Le Jossic-Corcos,C., Corcos,L. and Kornblihtt,A.R. (2014) How slow RNA polymerase II elongation favors alternative exon skipping. *Mol. Cell*, **54**, 683–690.
3. de la Mata,M., Alonso,C.R., Kadener,S., Fededa,J.P., Blaustein,M., Pelisch,F., Cramer,P., Bentley,D. and Kornblihtt,A.R. (2003) A slow RNA polymerase II affects alternative splicing in vivo. *Mol. Cell*, **12**, 525–532.
4. Schüller,R., Forné,I., Straub,T., Schreieck,A., Texier,Y., Shah,N., Decker,T.M., Cramer,P., Imhof,A. and Eick,D. (2016) Heptad-specific phosphorylation of RNA polymerase II CTD. *Mol. Cell*, **61**, 305–314.
5. Batsché,E., Yaniv,M. and Muchardt,C. (2006) The human SWI/SNF subunit Brm is a regulator of alternative splicing. *Nat. Struct. Mol. Biol.*, **13**, 22–29.
6. Nojima,T., Gomes,T., Grosso,A.R.F., Kimura,H., Dye,M.J., Dhir,S., Carmo-Fonseca,M. and Proudfoot,N.J. (2015) Mammalian NET-Seq reveals genome-wide nascent transcription coupled to RNA processing. *Cell*, **161**, 526–540.
7. Bartkowiak,B., Liu,P., Phatnani,H.P., Fuda,N.J., Cooper,J.J., Price,D.H., Adelman,K., Lis,J.T. and Greenleaf,A.L. (2010) CDK12 is a transcription elongation-associated CTD kinase, the metazoan ortholog of yeast Ctk1. *Genes Dev.*, **24**, 2303–2316.
8. Liang,K., Gao,X., Gilmore,J.M., Florens,L., Washburn,M.P., Smith,E. and Shilatifard,A. (2015) Characterization of human cyclin-dependent kinase 12 (CDK12) and CDK13 complexes in C-Terminal domain phosphorylation, gene transcription, and RNA processing. *Mol. Cell. Biol.*, **35**, 928–938.
9. Hintermair,C., Heidemann,M., Koch,F., Descostes,N., Gut,M., Gut,I., Fenouil,R., Ferrier,P., Flatley,A., Kremmer,E. *et al.* (2012) Threonine-4 of mammalian RNA polymerase II CTD is targeted by Polo-like kinase 3 and required for transcriptional elongation. *EMBO J.*, **31**, 2784–2797.
10. Di Vona,C., Bezdan,D., Islam,A.B., Salichs,E., López-Bigas,N., Ossowski,S. and de la Luna,S. (2015) Chromatin-wide profiling of DYRK1A reveals a role as a gene-specific RNA polymerase II CTD kinase. *Mol. Cell*, **57**, 506–520.
11. Yu,D., Cattoglio,C., Xue,Y. and Zhou,Q. (2019) A complex between DYRK1A and DCAF7 phosphorylates the C-terminal domain of RNA polymerase II to promote myogenesis. *Nucleic Acids Res.*, **47**, 4462–4475.
12. Devaiah,B.N., Lewis,B.A., Cherman,N., Hewitt,M.C., Albrecht,B.K., Robey,P.G., Ozato,K., Sims,R.J. 3rd and Singer,D.S. (2012) BRD4 is an atypical kinase that phosphorylates Serine2 of the RNA Polymerase II carboxy-terminal domain. *Proc. Natl. Acad. Sci. U.S.A.*, **109**, 6927–6932.
13. Uppal,S., Gegonne,A., Chen,Q., Meerzaman,D., Misra,H.S. and Singer,D.S. (2019) The bromodomain protein 4 contributes to the regulation of alternative splicing. *Cell Rep.*, **29**, 2450–2460.
14. Nemec,C.M., Singh,A.K., Ali,A., Tseng,S.C., Syal,K., Ringelberg,K.J., Ho,Y., Hintermair,C., Ahmad,M.F., Kar,R.K. *et al.* (2019) Noncanonical CTD kinases regulate RNA polymerase II in a gene-class-specific manner. *Nat. Chem. Biol.*, **15**, 123–131.
15. Muñoz,M.J., Pérez Santangelo,M.S., Paronetto,M.P., de la Mata,M., Pelisch,F., Boireau,S., Glover-Cutter,K., Ben-Dov,C., Blaustein,M., Lozano,J.J. *et al.* (2009) DNA damage regulates alternative splicing through inhibition of RNA Polymerase II Elongation. *Cell*, **137**, 708–720.
16. Williamson,L., Saponaro,M., Boeing,S., East,P., Mitter,R., Kantidakis,T., Kelly,G.P., Lobley,A., Walker,J., Spencer-Dene,B. *et al.* (2017) UV irradiation induces a Non-coding RNA that functionally opposes the protein encoded by the same gene. *Cell*, **168**, 843–855.
17. Tufegdžić Vidaković,A., Mitter,R., Kelly,G., Neumann,M., Harreman,M., Rodríguez-Martínez,M., Herlihy,A., Weems,J., Boeing,S., Encheva,V. *et al.* (2020) Regulation of the RNAPII pool is integral to the DNA damage response. *Cell*, **180**, 1245–1261.
18. Andrade-Lima,L.C., Veloso,A., Paulsen,M.T., Menck,C.F.M. and Ljungman,M. (2015) DNA repair and recovery of RNA synthesis following exposure to ultraviolet light are delayed in long genes. *Nucleic Acids Res.*, **43**, 2744–2756.
19. Tresini,M., Warmerdam,D.O., Kolovos,P., Snijder,L., Vrouwe,M.G., Demmers,J.A.A., Van Ijcken,W.F.J., Grosveld,F.G., Medema,R.H., Hoeijmakers,J.H. *et al.* (2015) The core spliceosome as target and effector of non-canonical ATM signalling. *Nature*, **523**, 53–58.
20. Muñoz,M.J., Nieto Moreno,N., Giono,L.E., Cambindo Botto,A.E., Dujardin,G., Bastianello,G., Lavore,S., Torres-Méndez,A., Menck,C.F.M., Blencowe,B.J. *et al.* (2017) Major roles for pyrimidine dimers, nucleotide excision repair, and ATR in the alternative splicing response to UV irradiation. *Cell Rep.*, **18**, 2868–2879.
21. Amente,S., Gargano,B., Napolitano,G., Lania,L. and Majello,B. (2009) Camptothecin releases P-TEFb from the inactive 7SK snRNP complex. *Cell Cycle*, **8**, 1249–1255.
22. Napolitano,G., Amente,S., Castiglia,V., Gargano,B., Ruda,V., Darzacq,X., Bensaude,O., Majello,B. and Lania,L. (2010) Caffeine

prevents transcription inhibition and P-TEFb/ 7SK dissociation following UV-Induced DNA damage. *PLoS One*, **5**, e11245.
23. Doble,B.W. and Woodgett,J. (2003) GSK-3: tricks of the trade for a multi-tasking kinase. *J. Cell Sci.*, **116**, 1175–1186.
24. Peterson,S.R., Dvir,A., Anderson,C.W. and Dynan,W.S. (1992) DNA binding provides a signal for phosphorylation of the RNA polymerase II heptapeptide repeats. *Genes (Basel)*, **6**, 426–438.
25. Luco,R.F., Pan,Q., Tominaga,K., Blencowe,B.J., Pereira-Smith,O.M. and Misteli,T. (2010) Regulation of alternative splicing by histone modifications. *Science*, **327**, 996–1001.
26. Ran,F.A., Hsu,P.D., Wright,J., Agarwala,V., Scott,D.A. and Zhang,F. (2013) Genome engineering using the CRISPR-Cas9 system. *Nat. Protoc.*, **8**, 2281–2308.
27. Orengo,J.P., Bundman,D. and Cooper,T.A. (2006) A bichromatic fluorescent reporter for cell-based screens of alternative splicing. *Nucleic Acids Res.*, **34**, e148.
28. Iizuka,R., Yamagishi-Shirasaki,M. and Funatsu,T. (2011) Kinetic study of de novo chromophore maturation of fluorescent proteins. *Anal. Biochem.*, **414**, 173–178.
29. Bevis,B.J. and Glick,B.S. (2002) Rapidly maturing variants of the Discosoma red fluorescent protein (DsRed). *Nat. Biotechnol.*, **20**, 83–87.
30. Ring,D.B., Johnson,K.W., Henriksen,E.J., Nuss,J.M., Goff,D., Kinnick,T.R., Ma,S.T., Reeder,J.W., Samuels,I., Slabiak,T. *et al.* (2003) Selective glycogen synthase kinase 3 inhibitors potentiate insulin activation of glucose transport and utilization in vitro and in vivo. *Diabetes*, **52**, 588–595.
31. Bhat,R., Xue,Y., Berg,S., Hellberg,S., Ormö,M., Nilsson,Y., Radesäter,A.C., Jerning,E., Markgren,P.O., Borgegård,T. *et al.* (2003) Structural insights and biological effects of glycogen synthase kinase 3-specific inhibitor AR-A014418. *J. Biol. Chem.*, **278**, 45937–45945.
32. Shinde,M.Y., Sidoli,S., Kulej,K., Mallory,M.J., Radens,C.M., Reicherter,A.L., Myers,R.L., Barash,Y., Lynch,K.W., Garcia,B.A. *et al.* (2017) Phosphoproteomics reveals that glycogen synthase kinase-3 phosphorylates multiple splicing factors and is associated with alternative splicing. *J. Biol. Chem.*, **292**, 18240–18255.
33. Ratner,J.N., Balasubramanian,B., Corden,J., Warren,S.L. and Bregman,D.B. (1998) Ultraviolet Radiation-induced Ubiquitination and proteasomal degradation of the large subunit of RNA Polymerase II. *J. Biol. Chem.*, **273**, 5184–5189.
34. Bataille,A.R., Jeronimo,C., Jaques,P.-É., Laramée,L., Fortin,M.-É., Forest,A., Bergeron,M., Hanes,S.D. and Robert,F. (2012) A universal RNA polymerase II CTD cycle is orchestrated by complex interplays between kinase, phosphatase, and isomerase enzymes along genes. *Mol. Cell*, **45**, 158–170.
35. Wang,H., Brown,J., Garcia,C.A., Tang,Y., Benakanakere,M.R., Greenway,T., Alard,P., Kinane,D.F. and Martin,M. (2011) The role of glycogen synthase kinase 3 in regulating IFN-β-Mediated IL-10 Production. *J. Immunol. Immunol.*, **186**, 675–684.
36. Doble,B.W., Patel,S., Wood,G.A., Kockeritz,L.K. and Woodgett,J.R. (2007) Functional Redundancy of GSK-3α and GSK-3β in Wnt/β-Catenin signaling shown by using an allelic series of embryonic stem cell lines. *Dev. Cell*, **12**, 957–971.
37. Lang,U., Kocabayoglu,P., Cheng,G., Ghiassi-Nejad,Z., Muñoz,U., Vetter,D., Eckstein,D., Hannivoort,R., Walsh,M. and Friedman,S. (2013) GSK3β phosphorylation of the KLF6 tumor suppressor promotes its transactivation of p21. *Oncogene*, **32**, 4557–4564.
38. Saldi,T., Fong,N. and Bentley,D.L. (2018) Transcription elongation rate affects nascent histone pre-mRNA folding and 3′ end processing. *Genes Dev.*, **32**, 297–308.
39. Wagner,F.F., Bishop,J.A., Gale,J.P., Shi,X., Walk,M., Ketterman,J., Patnaik,D., Barker,D., Walpita,D., Campbell,A.J. *et al.* (2016) Inhibitors of glycogen synthase kinase 3 with exquisite kinome-wide selectivity and their functional effects. *ACS Chem. Biol.*, **11**, 1952–1963.
40. Martinez,N.M., Agosto,L., Qiu,J., Mallory,M.J., Gazzara,M.R., Barash,Y., Fu,X. and Lynch,K.W. (2015) Widespread JNK-dependent alternative splicing induces a positive feedback loop through CELF2-mediated regulation of MKK7 during T-cell activation. *Genes Dev.*, **29**, 2054–2066.
41. Beurel,E., Grieco,S.F. and Jope,R.S. (2015) Glycogen synthase kinase-3 (GSK3): Regulation, actions, and diseases. *Pharmacol. Ther.*, **148**, 114–131.
42. Beurel,E. and Jope,R.S. (2006) The paradoxical pro- and anti-apoptotic actions of GSK3 in the intrinsic and extrinsic apoptosis signaling pathways. *Prog. Neurobiol.*, **79**, 173–189.
43. Maurer,U., Preiss,F., Brauns-Schubert,P., Schlicher,L. and Charvet,C. (2014) GSK-3 - at the crossroads of cell death and survival. *J. Cell Sci.*, **127**, 1369–1378.
44. Kurosu,T., Nagao,T., Wu,N., Oshikawa,G. and Miura,O. (2013) Inhibition of the PI3K/Akt/GSK3 pathway downstream of BCR/ABL, Jak2-V617F, or FLT3-ITD downregulates DNA damage-induced Chk1 activation as well as G2/M arrest and prominently enhances induction of apoptosis. *PLoS One*, **8**, e79478.
45. Beurel,E., Kornprobst,M., Blivet-Van Eggelpoël,M.J., Cadoret,A., Capeau,J. and Desbois-Mouthon,C. (2005) GSK-3β reactivation with LY294002 sensitizes hepatoma ells to chemotherapy-induced apoptosis. *Int. J. Oncol.*, **27**, 215–222.
46. Lee,J.Y., Yu,S.J., Park,Y.G., Kim,J. and Sohn,J. (2007) Glycogen synthase kinase 3β phosphorylates p21WAF1/CIP1 for proteasomal degradation after UV irradiation. *Mol. Cell. Biol.*, **27**, 3187–3198.
47. Watcharasit,P., Bijur,G.N., Zmijewski,J.W., Song,L., Zmijewska,A., Chen,X., Johnson,G.V.W. and Jope,R.S. (2002) Direct, activating interaction between glycogen synthase kinase-3β and p53 after DNA damage. *Proc. Natl. Acad. Sci. U.S.A.*, **99**, 7951–7955.
48. Patel,P. and Woodgett,J.R. (2017) Glycogen synthase kinase 3: A kinase for all pathways? *Curr. Top. Dev. Biol.*, **123**, 277–302.
49. Tejeda-Muñoz,N. and Robles-Flores,M. (2015) Glycogen synthase kinase 3 in Wnt signaling pathway and cancer. *IUBMB Life*, **67**, 914–922.